

Article

Electrocatalytic Oxidation of Cellulose to Gluconate on Carbon Aerogel Supported Gold Nanoparticles Anode in Alkaline Medium

Hanshuang Xiao, Meifen Wu and Guohua Zhao *

Received: 25 November 2015; Accepted: 25 December 2015; Published: 30 December 2015

Academic Editor: Rafael Luque

Department of Chemistry, Tongji University, Shanghai 200092, China; xhs@tongji.edu.cn (H.X.); wumf@tongji.edu.cn (M.W.)

* Correspondence: g.zhao@tongji.edu.cn; Tel.: +86-21-6598-1180; Fax: +86-21-6598-2287

Abstract: The development of high efficient and low energy consumption approaches for the transformation of cellulose is of high significance for a sustainable production of high value-added feedstocks. Herein, electrocatalytic oxidation technique was employed for the selective conversion of cellulose to gluconate in alkaline medium by using concentrated HNO₃ pretreated carbon aerogel (CA) supported Au nanoparticles as anode. Results show that a high gluconate yield of 67.8% and sum salts yield of 88.9% can be obtained after 18 h of electrolysis. The high conversion of cellulose and high selectivity to gluconate could be attributed to the good dissolution of cellulose in NaOH solution which promotes its hydrolysis, the surface oxidized CA support and Au nanoparticles catalyst which possesses high amount of active sites. Moreover, the bubbled air also plays important role in the enhancement of cellulose electrocatalytic conversion efficiency. Lastly, a probable mechanism for electrocatalytic oxidation of cellulose to gluconate in alkaline medium was also proposed.

Keywords: cellulose; alkaline condition; electrocatalytic oxidation; carbon aerogel supported Au nanoparticles; gluconate

1. Introduction

Cellulose, the most abundant source of biomass, is considered the most attractive alternative carbon source for the sustainable production of functionalized feedstocks since it is cheap, inedible and available on a large scale [1,2]. However, the transformation of cellulose into the specific chemicals is difficult because it owns low reactivity due to its crystalline fiber structure of β -1-4-glycosidic linkages in its long chains. Moreover, the network of intra- and intermolecular hydrogen bonds formed between the hydroxyl groups in adjacent cellulose makes it insoluble in water and in most organic solvents under mild conditions, which further aggravates the restriction for its utilization. In previous studies, various approaches including mineral acids hydrolysis, hydrothermal oxidation, enzymes hydrolysis, heterogeneous acids catalysis, metal and metal oxide catalysis, etc., were attempted to transform cellulose [3–8]. High value-added chemicals and fuels, such as glucose, polyols and organic acids, have been obtained. Among them, gluconic acid is an important industrial product, which can be usually used as water-soluble cleaner or as the additive in food and beverages. Wang *et al.* [9] performed the selective oxidation of cellobiose on Au nanoparticles supported on carbon nanotube (CNT) at 145 °C and 0.5 MPa O₂ and obtained an 80% yield to gluconic acid. In their study, the surface functional groups on CNT surfaces generated by pretreatment with HNO₃ is considered a key factor for the enhancement of the hydrolysis of cellobiose into glucose, while Au nanoparticles are attributed mainly to the oxidation of glucose into gluconic acid. An *et al.* [4] detected the oxidation of cellobiose to gluconic acid over polyoxometalate-supported Au nanoparticles. A 97% yield to gluconic acid was

achieved over Au/CS_{1.7}H_{1.3}PW₁₂O₄₀ at 145 °C and 0.5 MPa O₂, which was attributed to the high acidity of the catalyst. Moreover, the same catalyst afforded a 70% conversion of a ball-milled cellulose by oxidation at 145 °C under 1 MPa of O₂, resulting in a 60% yield to gluconic acid after 11 h. By using Au/TiO₂ as catalyst, Borgna *et al.* [7] achieved a 93% conversion of cellobiose and a 73.7% selectivity of gluconic acid. The high catalytic activity of Au/TiO₂ is considered to depend on the catalyst as a whole, especially the strong metal-support interaction between gold nanoparticles and titania support, rather than the sole size range of Au nanoparticles.

Electrocatalytic oxidation is another potential technique for biomass resource utilization due to its high reaction activity, low energy consumption and environmental compatibility. Many carbohydrates could be effectively transformed in an electrochemical system under mild conditions [10–15]. For example, the conversion of glucose can be performed through electrocatalytic oxidation obtaining a high selectivity to gluconic acid [16,17]. As we known, the glucose is a compulsory intermediate for the transformation of cellulose, thus it makes possible for the selective conversion of cellulose to gluconic acid in an electrocatalytic oxidation process. However, the investigations of cellulose directly transforming via electrocatalytic oxidation were still quite limited, which might be ascribed to the water insolubility of cellulose. Recently, alkaline aqueous solutions, such as NaOH, have been reported the novel green solvents of cellulose, which can dissolve cellulose by a freezing-thawing process [18]. Moreover, the dissolved cellulose has been revealed more readily to be hydrolyzed because of the broken of the intra- and inter-hydrogen bonding of cellulose [19]. Hence, we attempted to degrade the cellulose pretreated by concentrated NaOH solution through electrocatalytic oxidation in this study. Au nanoparticles supported on carbon aerogel (Au/CA) was designed as the electrocatalytic anode. Many studies indicated that Au nanoparticles, especially those with the size less than 10 nm, show superior catalytic performance and high selectivity in the conversion of cellobiose to gluconic acid [9,20]. Moreover, Au can be applied in an alkaline medium with a superior stability. The relatively high PH condition can even promote its catalytic activity [20,21]. While the CA support is selected not only by its good electrical conductivity but also by the excellent adsorption properties due to its high BET surface area and large pore volume [22]. Moreover, as a carbon support, it is expected to promote the cellulose hydrolyzing into glucose via the activation of β-1-4-glycosidic bond of cellulose, especially when the support was pretreated by concentrated mineral acid [9,23].

In this work, the properties of Au/CA electrocatalytic anode and the reaction condition were carefully investigated for exploring the high selective conversion efficiency of cellulose. Moreover, the main intermediates were also monitored with the variation of reaction time, which helps to understand the probable mechanism for the electrocatalytic oxidation of cellulose in alkaline condition.

2. Results and Discussion

2.1. Dissolution of Cellulose

Since cellulose is not dissolved in most solutions including water, which greatly inhibits its hydrolysis, the concentrated NaOH solution was used for the pretreatment of cellulose. Obviously, via a frozen-thawing process, the cellulose-NaOH solution presented a nearly homogeneous aqueous state (shown in Figure 1a). More dissolution information is included in supplementary information (Figure S1). Even Comparing with the XRD patterns for the dissolved and undissolved cellulose, Sugano, *et al.* [19] indicated that the intra- and inter-hydrogen bonding of cellulose are broken with the pretreatment of NaOH, which implies the cellulose molecular chain can migrate more easily in the solution and fully contact the catalytic electrode. Moreover, many studies also demonstrated that the hydrolysis of cellulose can be greatly promoted by the good dissolution of cellulose [19,24]. Deng *et al.* pointed out that the active sites of the glycosidic bond in dissolved cellulose can be more readily attacked and lead to the cellulose hydrolysis to glucose [25]. In an electrochemical oxidation system, sufficient ·O₂, ·OOH and chemisorbed active oxygen species are generated, which are proved

to be active radicals towards the hydrolysis of cellulose [11,14], suggesting efficient glucose might be produced in the cellulose-NaOH solution.

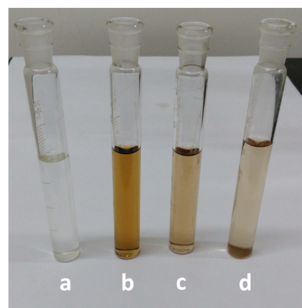


Figure 1. Photographs of cellulose solution: (a) Dissolved in NaOH solution; the products after electrolysis on; (b) Au/carbon aerogel (CA); (c) 50 nm-Au/CA; (d) Au/graphite.

2.2. Characterization of Electrocatalytic Anode

Figure 2 shows the SEM images of the CA support and Au/CA electrocatalyst. We can see that the used CA support has a loose interconnected 3D network structure consisting of granular carbon sphere with the pore size mainly in the range from several to a dozen nanometers. Au nanoparticles loaded are highly dispersed on the entire CA surface without aggregation. The further magnified image showed that the Au nanoparticles are mainly sphere structure with the uniform particles sizes of ~10 nm. The Au content determined by TG analysis is ~2% (as shown in Figure S2).

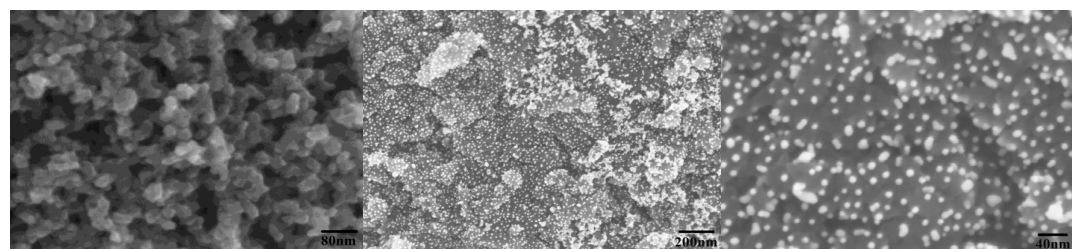


Figure 2. SEM images of (A) CA; (B) Au/CA; (C) magnification of Au/CA.

XRD patterns of the nanoparticles were obtained to investigate their phase and structure, as displayed in Figure 3a. The peaks at 22.1° and 43.2° were corresponded the typical characteristic peaks of CA [22]. Those at 38.1° , 44.4° , 64.6° and 77.6° are attributed to the {111}, {200}, {220} and {311} of Au, respectively. However, we can clearly see from Figure 3a, that Au/CA with the Au nanoparticle size of ~10 nm shows relatively diffuse diffractions compared to those in 50 nm-Au/CA, which are similar to the 9 nm-Au/C reported by Wang [26]. This might be ascribed to the presence of low lattice stabilized gold atoms or clusters of atoms. As we known, the atoms or atoms clusters with low lattice stability are usually considered active sites or hot spots, which afford good electrocatalytic activity [27]. According to the equation of Debye-Scherrer, a rough estimate based on the {111} peak indicates that the average size of Au nanoparticles along to the {111} lattice face is about 7.3 nm, in comparable with the result of the SEM measurement. In addition, XPS was also recorded for the as-prepared Au/CA to evaluate the chemical states of the different species. Figure 3b,c display the XPS spectra of the C_{1s} and Au_{4f} regions. From Figure 3b, we can see the C_{1s} peaks centered at 284.3 eV is corresponded to elemental carbon, while those at 285.5 and 288.2 eV are assigned to the oxygen bound species C-O and C=O, respectively [28]. While the peaks at 84.0 and 87.7 eV can be attributed to the 4f_{7/2} and 4f_{5/2}. It is reported that the 4f_{7/2} of Au⁰ and Au₂O₃ are located at 83.8 and 86.3 eV [9,28], respectively, suggesting the Au is approximately completely reduced.

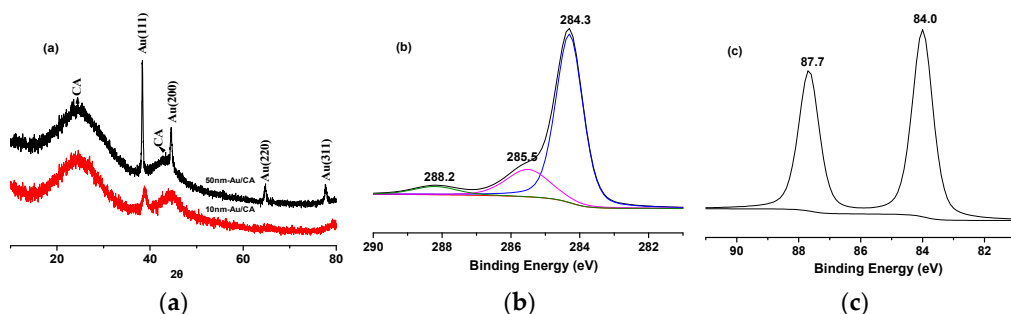


Figure 3. (a) X-ray diffraction (XRD) patterns of Au/CA and 50nm-Au/CA; (b) X-ray photoelectron spectrum analysis (XPS) of C_{1s}; (c) XPS of Au_{4f}.

2.3. Electrochemical Oxidation of Cellulose

The pretreated cellulose was subsequently transformed in the electrochemical system. To evaluate the efficiency of Au/CA, the Au/graphite and Au/CA in which the size of Au nanoparticles are ~50 nm were also used as anodes. Obviously, whatever the electrocatalysts selected, the brown solutions can be obtained after electrolysis with the decreased viscosity (Figure 1b–d). As neutralized by sulfuric acid solution, minor solids were found in the electrolyte from Au/graphite anode, suggesting the incomplete conversion of cellulose.

The liquids were then analyzed by HPLC. The observed oxidized products from electrolysis on different anodes are displayed in Table 1. Obviously, by using 10 nm-Au/CA as anode, the main product is gluconate (HPLC curve displayed in Figure S3) with the maximum yield reaching 67.8% after 18 h of electrolysis. Except for that, minor oxalate, formate and unidentified product was also detected, and the sum yield is ~89%. However, by using the Au/graphite or 50 nm-Au/CA as anode, the selectivity for gluconic acid is evidently decreased, accompanying with the increase of other small molecular organic acid salts such as glycolate and acetate. In addition, the sum yield of the produced organic acid salts was also prominently reduced as using Au/graphite to be the anode, which is only 52% after 18 h of electrolysis.

Table 1. Yield of organic acid salt from electrocatalytic oxidation on different anodes.

Electrocatalyst	Yield (%)					
	Gluconate	Glycolate	Acetate	Oxalate	Formate	Sum Yields
Au/graphite	32.7	5.4	4.3	6.5	3.4	52.3
50 nm-Au/CA	46.9	7.9	6.1	10.5	8.7	80.1
Au/CA	67.8	almost no	almost no	11.5	9.6	88.9

As we known, the catalytic activity of an electrocatalyst is affected not only by the nature of catalytic material, but also by the support properties. The support possessing high surface area and large pore volume can enhance the adsorption and mass transport of the reactants/intermediates during the reaction, which can greatly increase the conversion efficiency. Hence, by using N₂ adsorption-desorption, we detected the BET surface area and pore volume of the catalysts, as shown in Table 2. Clearly, we can see the CA support has a high BET surface area of 747 cm²·g⁻¹. With pretreated by concentrated HNO₃, the surface area of CA further increases and reaches 1004 cm²·g⁻¹, accompanying with the increase of pore volume from 0.4 to 0.52 m³·g⁻¹. Although the loading of Au nanoparticles leads to a decrease of the surface area and pore volume, it still reaches 499 m²·g⁻¹ and 0.45 cm³·g⁻¹, respectively, far high than those of Au/graphite. Besides that, the pretreatment of CA by concentrated HNO₃ can also introduce the surface functional groups on CA [29,30], which has been proved through the IR detections of CA with and without HNO₃ pretreatment (as shown in Figure S4). From Figure S4, a band at ~1631 cm⁻¹ is observed occurring in the spectrum of HNO₃

activated CA, assigned to COO^- group [30]. According to the references [9,31,32], surface oxidized carbons are promising water-tolerant materials that also demonstrated high catalytic performance for hydrolysis of cellulose or cellobiose. This might be attributed to its favorable adsorption to oxygen atoms of the 1-4-glycosidic bonds in cellulose molecules, so as to benefit the catalytic performance. Moreover, the introduce of surface oxidized functional groups to carbon support can also increase the interaction between Au nanoparticles and support, and at the same time, promote the selectivity of gluconic acid [7,9].

Table 2. Structure properties of the catalytic anodes.

Structure Properties	CA ^a	CA	Au/CA	Au/Graphite
BET surface area ($\text{cm}^2 \text{ g}^{-1}$)	747	1004	499	5.78
Pore volume ($\text{m}^3 \text{ g}^{-1}$)	0.40	0.52	0.45	-

^a CA support without the pretreatment by concentrated.

In addition, although Au is one of the most active electrocatalysts for the oxidation of cellulose [9,33], the high yield and high selectivity to gluconic acid (or gluconate) depends mainly on the size, dispersion and electronic state of Au. For the 50 nm-Au/CA anode, it obtained a high cellulose conversion; however, the selectivity of the gluconate is relatively lower, which might be ascribed to the larger size of Au nanoparticles. Several studies demonstrated that the Au nanoparticles with the diameter less than 10 nm have high performance of oxidation of glucose into gluconic acid [28,34,35]. In Au/CA electrode, the gold nanoparticles are highly dispersed on the surface of CA, with a uniform size of $\sim 10 \text{ }\mu\text{m}$, approving for its high efficiency.

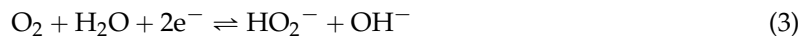
Considering that oxygen usually plays important roles in the selective oxidation of glucose to gluconic acid, particularly Au-based catalysts [4,7,28], the effect of oxygen was also studied on cellulose electrochemical oxidation by whether bubbling air into the reaction system or not. Experiment results show that the products of cellulose electrolysis are constant regardless of with or without air aeration, accompanying with a nearly unchanged products distribution. However, the aeration of air can evidently increase the reaction rate. From Figure 4, we can see, after 18 h electrolysis, the gluconic acid yield and sum acids yield are 49.6% and 68.2%, respectively, as no air aeration, while those reach 67.8% and 88.9%, respectively, with bubbling of air. In the degradation of the lignin by PbO_2/Pb anode, Zhang *et al.* [11] considered the insufflated air enhances the conversion of O_2 to superoxide anion radical (O_2^-) on cathode surface, leading to a higher efficiency for lignin transformation. Burke and Nugent [36] studied the electrochemistry of gold and concluded that the dissolved oxidant can induce Au to form AuO_x at active sites, which often act as the mediators for oxidation reaction. While the monomeric Au(III) hydroxyl complexes of the form Au(OH)_6^{3-} is proposed by Doyle and Lyons [37]. Moreover, the increment of oxygen can also effectively increase the O_2 adsorption on Au surfaces by forming linear O–Au–O structure, contributing to the high catalysis efficiency of gold [38,39]. Hence, the aeration of air is deduced to increase the active Au-oxide species resulting in a better transformation of cellulose. More importantly, the aeration of air can accelerate the cathode reaction. It is known that, in alkaline media, H_2O and dissolved oxygen are the possible reductions which can be reduced at cathode. As H_2O acts as the reductant, it reacts via the hydrogen evolution reaction:



As oxygen acting as the reductant, it is generally reduced via two pathways [40,41], *i.e.*, a four-electron pathway leading directly to OH^- , expressed as:



or a two-electron pathway with hydrogen peroxide (HO_2^- in alkaline media) as the intermediate:



whether the reduction of oxygen to OH^- or to HO_2^- , it is relatively easier than water to hydrogen in an alkaline condition because it requires a more negative potential [41,42]. Moreover, the reduction of oxygen is, to some extent, limited by its transport rate to the cathode. With bubbling into air, the transport of oxygen can be greatly accelerated, which can effectively increase the reduction reaction rate at cathode, resulting in the promotion of reaction efficiency.

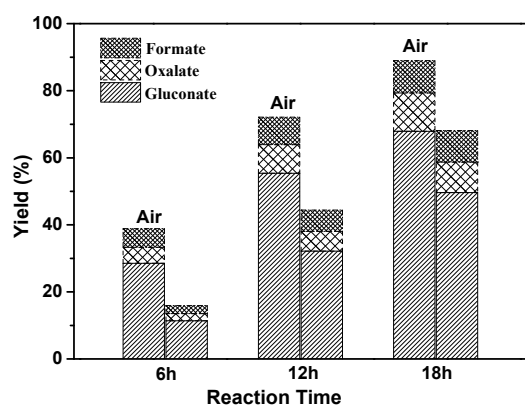


Figure 4. Yield of organic acid salt from electrocatalytic oxidation of cellulose on Au/CA anode with and without air bubbled in reaction system.

For better understanding the mechanism of cellulose oxidation on Au/CA anode, the intermediates were monitored by HPLC with variation of reaction time. Figure 5 shows the yields of gluconate, oxalate and formate, respectively, at different the reaction time. It can be observed that gluconate was produced rapidly in the initial 10 h, and then it increased at a slightly reduced rate till it reached the maximum yield of 67.8% at 18 h. Continuously increasing the reaction time, the concentration of gluconate was decreased, accompanying with the evident concentration increases of oxalate, implying the oxalate might be the product for gluconate deep oxidation. Thus, a probable mechanism for electrocatalytic oxidation of cellulose to gluconate in an alkaline condition can be proposed as Scheme 1.

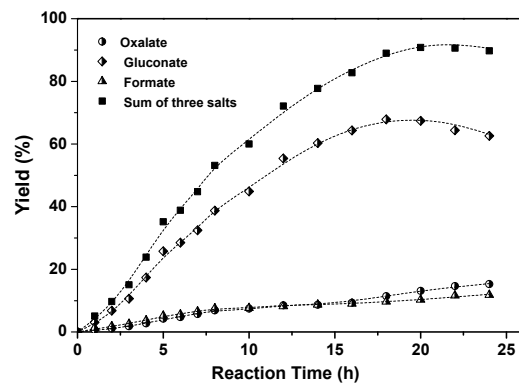
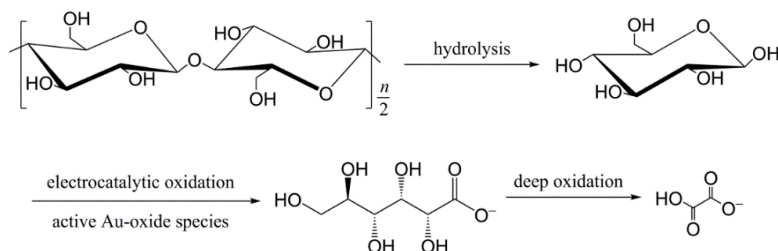


Figure 5. Yield of organic acid salt from electrocatalytic oxidation of cellulose on Au/CA anode varied with reaction time.



Scheme 1. Mechanism for electrocatalytic oxidation of cellulose to gluconate.

As for formate, it displays an inconspicuous increase with the decomposition of gluconate, deduced likely to be the direct oxidation of glucose via α -scission [24,43]. In addition, the total yield of gluconate, oxalate and formate is also calculated and shown in Figure 5. Surprisingly, the sum yields were very high with the value of ~91% at the reaction time of 22 h, implying the high conversion efficiency of cellulose on Au/CA anode in alkaline condition.

3. Experimental Section

3.1. Materials

Cellulose and HAuCl₄·4H₂O were purchased from Sigma-Aldrich (Shanghai, China). Other chemicals used were analytical grade. All solutions were prepared with deionized water.

3.2. Pretreatment of Cellulose

Before the electrochemical oxidization process, 1 g cellulose was dissolved in 133.3 mL NaOH solution (0 °C, 12 wt. %) under stirring at 1000 rpm for 2 h, and then the suspension was stored at -20 °C for 24 h. The frozen sample was consequently thawed at room temperature and diluted with deionized water to the volume of 200 mL. Thus, final concentration of cellulose in NaOH solution was 5 g L⁻¹.

3.3. Preparation of Au/CA Electrode

CA support is fabricated with the method reported in our previous study [22]. Briefly, resorcinol, formaldehyde, deionized water and sodium carbonate were mixed with a fixed molar ratio forming a homogeneous solution, which is then sealed into a cuboid glass reactor and cured at 30, 50 and 90 °C, separately, to obtain organic wet gel. The as-prepared gel was dried via solvent exchange in acetone under ambient condition and then carbonized in a tubular oven at 950 °C for 4 h in nitrogen atmosphere to convert to CA. Before loading Au nanoparticles, the CA was pretreated by 68% HNO₃ at room temperature for 24 h.

The Au/CA electrode was prepared by using the improved method from Ma, *et al.* [28]. A solution was mixed with HAuCl₄ (0.39 mg Au mL⁻¹) and 2 wt. % PVP with vigorous stirring. To this solution, a freshly prepared NaBH₄ solution was added dropwise, with a NaBH₄/Au molar ratio of 4. This process is performed in an ice-water condition, which lead to the formation of Au nanoparticles with a moderate reaction rate. The immobility of Au nanoparticles was achieved by repeatedly immersing the pretreated CA into the mixed solution for 10 min and then drying at 70 °C for 30 min for 5 times. Finally, the as-prepared Au/CA catalyst was washed by deionized water fully and dried at 70 °C for 5 h, then calcined at 200 °C for 3 h. For the purpose of comparison, Au/graphite catalyst was prepared with the same method mentioned above, and the Au nanoparticles with a size of about 50 nm were also prepared and deposited on CA with a HAuCl₄ concentration of 0.59 mg Au mL⁻¹ and the same method.

3.4. Catalyst Characterization

Surface morphology of the catalyst was determined by scanning electron microscopy (FESEM, Hitach S-4800, Tokyo, Japan) equipped with energy-dispersive X-ray spectrometer (EDS). The surface area and pore size of the catalysts were carried out by nitrogen adsorption at 77 K using BET analyzer (Micromeritics Tristar 3000, Norcross, GA, USA). The Au content was determined with thermogravimetric analysis (TG/DSC, NETZSCH STA 409PC, Bavaria, Germany). The crystallographic structure was determined by X-ray diffraction (XRD, Bruker D8, saarbrücken, Germany) with Cu K α ($\lambda = 0.154056$ nm) at a voltage of 40 KV, a current of 40 mA, and a scanning rate of 0.02 step/s. The surface properties of the catalyst were detected by X-ray photoelectron spectrum analysis (XPS, Shimadzu Axis-Ultra DLD, Manchester, Britain) with Mg K α X-rays radiation ($H_v = 1253.6$ eV). In addition, cyclic voltammetry (CV) was measured by Electrochemical Workstation (CHI660, Chenhua, Shanghai, China) for obtaining the electrochemical properties of cellulose solution on Au nanoparticles electrodes with the results displaying in Figures S5 and S6.

3.5. Electro-Oxidation Reaction

The electrocatalytic oxidation of cellulose was carried out in a cylindrical single compartment cell system equipped with air-blowing device. The constructed Au/CA electrode with an area of 4 cm^2 was used as anode and a Pt sheet with the same area was used as cathode. The gap of electrodes between electrodes was 1 cm. The current density used was controlled at 10 mA cm^{-2} with a cell voltage of ~ 2.75 V. Air was bubbled into the reaction system at a flow rate of 150 mL min^{-1} . Each time, a 50 mL pretreated cellulose solution was used for transformed.

3.6. Products Analysis

After reaction, the alkaline liquid was adjusted by sulfuric acid to pH = 2. Then it was syringe filtered with $0.45\text{ }\mu\text{m}$ PTFE membrane and analyzed by a high-performance liquid chromatography (HPLC, Agilent 1260, Santa Clara, CA, USA) on an Agilent Hi-plex H column at a UV detection wavelength of 210 nm. The mobile phases are using 5 mM sulfuric acid solution with a flow rate of 0.6 mL min^{-1} and the injection condition is $55\text{ }^\circ\text{C}$.

4. Conclusions

In this work, the electrocatalytic oxidation of cellulose was performed on the concentrated HNO_3 pretreated CA supported Au nanoparticles anode in an alkaline medium with the aeration of air. Results show that cellulose can be effectively degraded on Au/CA anode and a high gluconate yield of 67.8% can be obtained after 18 h of electrolysis. The high conversion of cellulose and high selectivity to gluconic acid could be attributed not only to the properties of Au nanoparticles but also the CA support. Moreover, the dissolution of cellulose in NaOH solution can promote the hydrolysis of cellulose, which also plays important role in the cellulose conversion. Additionally, a probable mechanism for electrocatalytic oxidation of cellulose to gluconate in an alkaline condition was also proposed.

Acknowledgments: This work was supported by the National Natural Science Foundation of China (NO. 51208367, 21477085).

Author Contributions: The experimental work was conceived and designed by Guohua Zhao and Hanshuang Xiao, Hanshuang Xiao performed the experiments; Hanshuang Xiao and Meifen Wu analyzed the data and Hanshuang Xiao drafted the paper. The manuscript was amended through the comments of all authors. All authors have given approval for the final version of the manuscript.

Conflicts of Interest: The authors declare no conflict of interest.

References

1. Besson, M.; Gallezot, P.; Pinel, C. Conversion of Biomass into Chemicals over Metal Catalysts. *Chem. Rev.* **2014**, *114*, 1827–1870. [[CrossRef](#)] [[PubMed](#)]
2. Wang, L.; Xiao, F.S. Nanoporous catalysts for biomass conversion. *Green Chem.* **2015**, *17*, 24–39. [[CrossRef](#)]
3. Krochta, J.M.; Hudson, J.S. Alkaline thermochemical degradation of rice straw to organic acids. *Agric. Wastes* **1985**, *14*, 243–254. [[CrossRef](#)]
4. An, D.L.; Ye, A.H.; Deng, W.P.; Zhang, Q.H.; Wang, Y. Selective Conversion of Cellobiose and Cellulose into Gluconic Acid in Water in the Presence of Oxygen, Catalyzed by Polyoxometalate-Supported Gold Nanoparticles. *Chem. Eur. J.* **2012**, *18*, 2938–2947. [[CrossRef](#)] [[PubMed](#)]
5. Saxena, R.C.; Adhikari, D.K.; Goyal, H.B. Biomass-based energy fuel through biochemical routes: A review. *Renew. Sustain. Energy Rev.* **2009**, *13*, 167–178. [[CrossRef](#)]
6. Deng, W.P.; Zhang, Q.H.; Wang, Y. Catalytic transformations of cellulose and cellulose-derived carbohydrates into organic acids. *Catal. Today* **2014**, *234*, 31–41. [[CrossRef](#)]
7. Amaniampong, P.N.; Li, K.; Jia, X.; Wang, B.; Borgna, A.; Yang, Y. Titania-Supported Gold Nanoparticles as Efficient Catalysts for the Oxidation of Cellobiose to Organic Acids in Aqueous Medium. *ChemCatChem* **2014**, *6*, 2105–2114. [[CrossRef](#)]
8. Cantero, D.A.; Martinez, C.; Bermejo, M.D.; Cocero, M.J. Simultaneous and selective recovery of cellulose and hemicellulose fractions from wheat bran by supercritical water hydrolysis. *Green Chem.* **2015**, *17*, 610–618. [[CrossRef](#)]
9. Tan, X.S.; Deng, W.P.; Liu, M.; Zhang, Q.H.; Wang, Y. Carbon nanotube-supported gold nanoparticles as efficient catalysts for selective oxidation of cellobiose into gluconic acid in aqueous medium. *Chem. Commun.* **2009**, 7179–7181. [[CrossRef](#)] [[PubMed](#)]
10. Yu, J.C.; Bauzer, M.M.; Nobe, K. Electrochemical Generated Acid Catalysis of Cellulose Hydrolysis. *J. Electrochem. Soc.* **1986**, *135*, 83–87. [[CrossRef](#)]
11. Zhang, Y.M.; Peng, Y.; Yin, X.L.; Liu, Z.H.; Li, G. Degradation of lignin to BHT by electrochemical catalysis on Pb/PbO₂ anode in alkaline solution. *J. Chem. Technol. Biotechnol.* **2014**, *89*, 1954–1960. [[CrossRef](#)]
12. Yang, F.; Zhang, Q.; Fan, H.X.; Li, Y.; Li, G. Electrochemical control of the conversion of cellulose oligosaccharides into glucose. *J. Ind. Eng. Chem.* **2014**, *20*, 3487–3492. [[CrossRef](#)]
13. Xin, L.; Zhang, Z.Y.; Qi, J.; Chadderdon, D.; Li, W.Z. Electrocatalytic oxidation of ethylene glycol (EG) on supported Pt and Au catalysts in alkaline media: Reaction pathway investigation in three-electrode cell and fuel cell reactors. *Appl. Catal. B* **2012**, *125*, 85–94. [[CrossRef](#)]
14. Kwon, Y.; Kleijn, S.E.F.; Schouten, K.J.P.; Koper, M.T.M. Cellobiose hydrolysis and decomposition by electrochemical generation of acid and hydroxyl radicals. *ChemSusChem* **2012**, *5*, 1935–1943. [[CrossRef](#)] [[PubMed](#)]
15. Meng, D.F.; Li, G.; Liu, Z.H.; Yang, F. Study of depolymerization of cotton cellulose by Pb/PbO₂ anode electrochemical catalysis in sulfuric acid solution. *Polym. Degrad. Stab.* **2011**, *96*, 1173–1178. [[CrossRef](#)]
16. Delidovich, I.V.; Moroz, B.L.; Taran, O.P.; Gromov, N.K.; Pyrjaev, P.A.; Prosvirin, I.P.; Bukhtiyarov, V.I.; Parmon, V.N. Aerobic selective oxidation of glucose to gluconate catalyzed by Au/Al₂O₃ and Au/C: Impact of the mass-transfer processes on the overall kinetics. *Chem. Eng. J.* **2013**, *223*, 921–931.
17. Pasta, M.; Mantia, F.L.; Cui, Y. Mechanism of glucose electrochemical oxidation on gold surface. *Electrochem. Acta* **2010**, *55*, 5561–5568. [[CrossRef](#)]
18. Duchemin, B.J.C. Mercerisation of cellulose in aqueous NaOH at low concentrations. *Green Chem.* **2015**, *17*, 3941–3947. [[CrossRef](#)]
19. Sugano, Y.; Vestergaard, M.; Yoshikawa, H.; Saito, M.; Tamiya, E. Direct Electrochemical Oxidation of Cellulose: A Cellulose-Based Fuel Cell System. *Electroanalysis* **2010**, *22*, 1688–1694. [[CrossRef](#)]
20. Zhang, J.Z.; Liu, X.; Hedhili, N.J.; Zhu, Y.H.; Han, Y. Highly Selective and Complete Conversion of Cellobiose to Gluconic Acid over Au/Cs₂HPW₁₂O₄₀ Nanocomposite Catalyst. *ChemCatChem* **2011**, *3*, 1294–1298. [[CrossRef](#)]
21. Biella, S.; Prati, L.; Rossi, M. Selective oxidation of D-glucose on gold catalyst. *J. Catal.* **2002**, *206*, 242–247. [[CrossRef](#)]

22. Wu, M.F.; Jin, Y.N.; Zhao, G.H.; Li, M.F.; Li, D.M. Electrosorption-promoted Photodegradation of Opaque Wastewater on A Novel TiO₂/Carbon Aerogel Electrode. *Environ. Sci. Technol.* **2010**, *44*, 1780–1785. [CrossRef] [PubMed]
23. Komanoya, T.; Kobayashi, H.; Hara, K.; Chun, W.J.; Fukuoka, A. Catalysis and characterization of carbon-supported ruthenium for cellulose hydrolysis. *Appl. Catal. A* **2011**, *407*, 188–194. [CrossRef]
24. Deng, W.P.; Zhang, Q.H.; Wang, Y. Catalytic transformations of cellulose and its derived carbohydrates into 5-hydroxymethylfurfural, levulinic acid, and lactic acid. *Sci. China Chem.* **2015**, *58*, 29–46. [CrossRef]
25. Yan, L.F.; Qi, X.Y. Degradation of Cellulose to Organic Acids in its Homogeneous Alkaline Aqueous Solution. *ACS Sustain. Chem. Eng.* **2014**, *2*, 897–901. [CrossRef]
26. Wang, S.; Zhao, Q.; Wei, H.; Wang, J.Q.; Cho, M.; Cho, H.; Terasaki, O.; Wan, Y. Aggregation-Free Gold Nanoparticles in Ordered Mesoporous Carbons: Toward Highly Active and Stable Heterogeneous Catalysts. *J. Am. Chem. Soc.* **2013**, *135*, 11849–11860. [CrossRef] [PubMed]
27. Plowman, B.J.; O'Mullane, A.P.; Bhargava, S.K. The active site behaviour of electrochemically synthesised gold nanomaterials. *Faraday Discuss.* **2011**, *152*, 43–62. [CrossRef] [PubMed]
28. Ma, C.Y.; Xue, W.J.; Li, J.J.; Xing, W.; Hao, Z.P. Mesoporous carbon-confined Au catalysts with superior activity for selective oxidation of glucose to gluconic acid. *Green Chem.* **2013**, *15*, 1035–1041. [CrossRef]
29. Ruffo, M.P.R.; Falletta, E.; Mari, C.M.; Pina, C.D. Alkaline glucose oxidation on nanostructured gold electrodes. *Gold Bullet.* **2010**, *43*, 57–64.
30. Wu, C.; Yan, P.T.; Zhang, R.J.; Jin, J.L.; Zhang, X.H.; Kang, H.M. Comparative study of HNO₃ activation effect on porous carbons having different porous characteristics. *J. Appl. Electrochem.* **2015**, *45*, 849–856. [CrossRef]
31. Zhao, X.; Wang, J.; Chen, C.; Huang, Y.; Wang, A.; Zhang, T. Graphene oxide for cellulose hydrolysis: How it works as a highly active catalyst? *Chem. Commun.* **2014**, *50*, 3439–3442. [CrossRef] [PubMed]
32. Delidovich, I.; Palkovits, R. Impacts of acidity and textural properties of oxidized carbon materials on their catalytic activity for hydrolysis of cellobiose. *Microporous Mesoporouws Mater.* **2016**, *219*, 317–321. [CrossRef]
33. Sugano, Y.; Latonen, R.M.; Akieh-Pirkanniemi, M.; Bobacka, J.; Ivaska, A. Electrocatalytic Oxidation of Cellulose at a Gold Electrode. *ChemSusChem* **2014**, *7*, 2240–2247. [CrossRef] [PubMed]
34. Qi, P.Y.; Chen, S.S.; Chen, J.; Zheng, J.W.; Zheng, X.L.; Yuan, Y.Z. Catalysis and Reactivation of Ordered Mesoporous Carbon-Supported Gold Nanoparticles for the Base-Free Oxidation of Glucose to Gluconic Acid. *ACS Catal.* **2015**, *5*, 2659–2670. [CrossRef]
35. Ishimotoa, T.; Hamatake, Y.; Azunob, H.; Kishidab, T.; Koyamaa, M. Theoretical study of support effect of Au catalyst for glucose oxidation of alkaline fuel cell anode. *Appl. Surf. Sci.* **2015**, *324*, 76–81. [CrossRef]
36. Burke, L.D.; Nugent, P.F. The electrochemistry of gold: II The electrocatalytic behavior of the metal in aqueous media. *Gold Bullet.* **1998**, *31*, 39–50. [CrossRef]
37. Doyle, R.; Lyons, M.E. The mechanism of oxygen evolution at superactivated gold electrodes in aqueous alkaline solution. *J. Solid State Electrochem.* **2014**, *18*, 3271–3286. [CrossRef]
38. Sun, K.; Kohyama, M.; Tanaka, S.; Takeda, S. Direct O₂ Activation on Gold/Metal Oxide Catalysts through a Unique Double Linear O–Au–O Structure. *ChemCatChem* **2013**, *5*, 2217–2222. [CrossRef]
39. Sun, K.; Kohyama, M.; Tanaka, S.; Takeda, S. Theoretical Study of Atomic Oxygen on Gold Surface by Hückel Theory and DFT Calculations. *J. Phys. Chem. A* **2012**, *116*, 9568–9573. [CrossRef] [PubMed]
40. Genies, L.; Bultel, Y.; Faure, R.; Durand, R. Impedance study of the oxygen reduction reaction on platinum nanoparticles in alkaline media. *Electrochimica Acta* **2003**, *48*, 3879–3890. [CrossRef]
41. Ge, X.M.; Sumboja, A.; Wuu, D.; An, T.; Li, B.; Goh, F.W.T.; Hor, T.S.A.; Zong, Y.; Liu, Z.L. Oxygen Reduction in Alkaline Media: From Mechanisms to Recent Advances of Catalysts. *ACS Catal.* **2015**, *5*, 4643–4667. [CrossRef]
42. Shinagawa, T.; Garcia-Esparza, A.T.; Takanabe, K. Mechanistic Switching by Hydronium Ion Activity for Hydrogen Evolution and Oxidation over Polycrystalline Platinum Disk and Platinum/Carbon Electrodes. *ChemElectroChem* **2014**, *1*, 1497–1507. [CrossRef]
43. Jin, F.M.; Yun, J.; Li, G.M.; Kishita, A.; Tohji, K.; Enomoto, H. Hydrothermal conversion of carbohydrate biomass into formic acid at mild temperatures. *Green Chem.* **2008**, *10*, 612–615. [CrossRef]

